



# MIT Open Access Articles

## *Multidimensional chemical control of CRISPR-Cas9*

The MIT Faculty has made this article openly available. **Please share** how this access benefits you. Your story matters.

<b>Citation</b>	Maji, Basudeb et al. "Multidimensional chemical control of CRISPR-Cas9." Nature Chemical Biology 13 (January 2017): 9-11 © 2016 The Author(s)
<b>As Published</b>	<a href="http://dx.doi.org/10.1038/NCHEMBIO.2224">http://dx.doi.org/10.1038/NCHEMBIO.2224</a>
<b>Publisher</b>	Nature Publishing Group
<b>Version</b>	Author's final manuscript
<b>Citable link</b>	<a href="http://hdl.handle.net/1721.1/112729">http://hdl.handle.net/1721.1/112729</a>
<b>Terms of Use</b>	Creative Commons Attribution-Noncommercial-Share Alike
<b>Detailed Terms</b>	<a href="http://creativecommons.org/licenses/by-nc-sa/4.0/">http://creativecommons.org/licenses/by-nc-sa/4.0/</a>



# HHS Public Access

Author manuscript

*Nat Chem Biol.* Author manuscript; available in PMC 2017 July 27.

Published in final edited form as:

*Nat Chem Biol.* 2017 January ; 13(1): 9–11. doi:10.1038/nchembio.2224.

## Multidimensional chemical control of CRISPR–Cas9

**Basudeb Maji**<sup>1,2,3,8</sup>, **Christopher L Moore**<sup>1,4,8</sup>, **Bernd Zetsche**<sup>1,5,6,7</sup>, **Sara E Volz**<sup>1,5,6,7</sup>, **Feng Zhang**<sup>1,5,6,7</sup>, **Matthew D Shoulders**<sup>1,4,\*</sup>, and **Amit Choudhary**<sup>1,2,3,\*</sup>

<sup>1</sup>Broad Institute of MIT and Harvard, Cambridge, Massachusetts, USA

<sup>2</sup>Department of Medicine, Harvard Medical School, Boston, Massachusetts, USA

<sup>3</sup>Renal Division, Brigham and Women's Hospital, Boston, Massachusetts, USA

<sup>4</sup>Department of Chemistry, Massachusetts Institute of Technology, Cambridge, Massachusetts, USA

<sup>5</sup>McGovern Institute for Brain Research, Massachusetts Institute of Technology, Cambridge, Massachusetts, USA

<sup>6</sup>Department of Brain and Cognitive Sciences, Massachusetts Institute of Technology, Cambridge, Massachusetts, USA

<sup>7</sup>Department of Biological Engineering, Massachusetts Institute of Technology, Cambridge, Massachusetts, USA

### Abstract

Cas9-based technologies have transformed genome engineering and the interrogation of genomic functions, but methods to control such technologies across numerous dimensions—including dose, time, specificity, and mutually exclusive modulation of multiple genes—are still lacking. We conferred such multidimensional controls to diverse Cas9 systems by leveraging small-molecule-regulated protein degron domains. Application of our strategy to both Cas9-mediated genome editing and transcriptional activities opens new avenues for systematic genome interrogation.

---

RNA-guided endonucleases, such as Cas9, can be easily targeted to any genomic locus through the use of single guide RNAs (sgRNAs)<sup>1,2</sup>, ushering in a slew of transformative technologies. For example, Cas9 enables facile genomic alterations, as well as robust self-propagation of such alterations throughout a species population via gene drives<sup>3</sup>.

---

Reprints and permissions information is available online at <http://www.nature.com/reprints/index.html>.

\* mshoulde@mit.edu or achoud@broadinstitute.org.

<sup>8</sup>These authors contributed equally to this work.

Correspondence and requests for materials should be addressed to M.D.S. or A.C

#### Author contributions

B.M., C.L.M., B.Z., M.D.S., and A.C. planned research and analyzed data; B.M., C.L.M., B.Z., F.Z., M.D.S., and A.C. designed experiments; B.M., C.L.M., B.Z., and S.E.V. performed experiments; B.M., C.L.M., M.D.S., and A.C. wrote the manuscript; M.D.S. and A.C. supervised research.

#### Competing financial interests

The authors declare competing financial interests: details are available in the online version of the paper.

#### Additional information

Any supplementary information, chemical compound information and source data are available in the online version of the paper.

Furthermore, catalytically inactive Cas9 (dCas9) can be fused to a wide range of effectors, such as fluorescent proteins for genome imaging<sup>4</sup>, enzymes that modify DNA or histones for epigenome editing<sup>5</sup>, and transcription-regulating domains for controlling endogenous gene expression<sup>6</sup>.

Despite such advances, a need exists for methods to precisely regulate Cas9 activities across multiple dimensions, including dose, target, and time<sup>7</sup>. Finely tuned control of Cas9 levels is important<sup>8</sup>, as high Cas9 leads to elevated off-target genomic alterations. Rapid disabling of Cas9 activity after a desired genomic modification is also valuable to prevent off-target activity<sup>9</sup>. In the context of gene regulation by dCas9-based transcriptional activators, dose-based control of transcript expression is essential to permit induction of physiologically relevant levels of mRNA transcripts. Capability to rapidly reverse transcript induction and to control the expression of multiple transcripts independently is also highly desirable. Ideally, methods that provide such controls should be readily adaptable to newly emerging RNA-guided nucleases.

We sought small-molecule-regulated systems that would fulfill these needs. Previously, we applied destabilized domains (DDs)<sup>10–12</sup> to confer similar controls on transcription factors<sup>13,14</sup>. Briefly, structurally unstable protein domains derived from *Escherichia coli* dihydrofolate reductase (DHFR)<sup>10</sup> or the estrogen receptor (ER50)<sup>11</sup> are fused to a transcription factor. These largely unfolded domains target the fusion protein for rapid proteasomal degradation. Small molecules that can bind and stabilize the DDs in their poorly populated folded state prevent proteasomal degradation of the fusion protein in a concentration-dependent manner, allowing transcription factor function<sup>13,14</sup>. We envisioned that such small-molecule-regulated DDs could be similarly deployed to establish Cas9 systems with multidimensional control of genome editing and transcriptional activities.

We began by linking the DHFR DD to the N terminus of catalytically inactive *Streptococcus pyogenes* Cas9 (dSpCas9) fused to a VP16-based transcriptional activation domain (e.g., VP64 or VP192)<sup>15</sup>. The addition of trimethoprim (TMP), a DHFR-stabilizing small molecule, to cells transfected with either DHFR.dSpCas9.VP64 or a DHFR.dSpCas9.VP192 fusion construct<sup>16</sup> and appropriate sgRNAs yielded minimal induction of target genes or high basal activity (Supplementary Results, Supplementary Fig. 1). These findings were expected, as dSpCas9.VP64 alone is insufficient for inducing the transcription of many target genes<sup>17</sup>.

We shifted our focus to a second-generation Cas9-based transcription system<sup>17</sup> in which sgRNAs bear an RNA aptamer that recruits transcription activation domains (e.g., PP7.VP64 (ref. 18)) to dSpCas9. We imparted conditional activity to this system by fusing the DHFR DD to the PP7.VP64 transcription activation domain (Fig. 1a). Cells transiently expressing DHFR.PP7.VP64, dSpCas9, and an sgRNA targeting *ILIRN* showed robust upregulation of *ILIRN* mRNA after treatment with TMP, demonstrating ‘chemical’ control of transcript induction (Fig. 1a and Supplementary Fig. 2). Importantly, we observed minimal basal transcriptional activation in vehicle-treated samples.

Existing small-molecule-regulated dCas9 transcriptional activators leave transcription continuously on<sup>7,19</sup>, in contrast to biological systems in which both activation and cessation of transcription are often strictly regulated. An advantage of our approach is the potential for turning off transcription after removal of the DD-stabilizing small molecule. We treated cells transfected with DHFR.PP7.VP64, dSpCas9, and sgRNA with TMP to upregulate endogenous genes before a chase period with media lacking TMP (Fig. 1b). Removal of TMP resulted in rapid depletion of induced mRNA transcript levels within <8 h for multiple genes (Fig. 1b and Supplementary Fig. 3). Thus, our system was shown to permit user-defined turn-on and turn-off of endogenous gene transcription.

Another attractive feature of our strategy is that several orthogonal small molecule–degron pairs exist<sup>10,11</sup>, theoretically enabling independent control of the transcription of multiple genes. For example, the ER50 DD stabilized by the small molecule (*Z*)-4-hydroxytamoxifen (4OHT)<sup>11</sup> is orthogonal to the TMP–DHFR pair. Conveniently, the cognate RNA aptamer of the transcription activation domain MS2.p65.HSF1 is distinct from that bound by the PP7.VP64 domain, and therefore MS2.p65.HSF1 is functionally orthogonal to PP7.VP64 (refs. 17,18). Similar to our previous observations in experiments with DHFR.PP7.VP64 and TMP, expression of ER50.MS2.p65.HSF1 with dSpCas9 and an appropriate sgRNA yielded 4OHT-dependent transcript induction (Fig. 1c). Immunoblotting confirmed that this induction was accompanied by a 4OHT-dependent increase in the amount of ER50.MS2.p65.HSF1 protein (Supplementary Fig. 4). As expected, we observed a similar increase in amounts of ER50.MS2.p65.HSF1 protein after proteasome inhibition using MG-132, confirming that 4OHT rescues the transcription activation domain from degradation (Supplementary Fig. 4). Most important, co-expression of both DHFR.PP7.VP64 and ER50.MS2.p65.HSF1, along with dSpCas9 and appropriate sgRNAs, permitted conditional and orthogonal activation of multiple endogenous genes when TMP, 4OHT, or both TMP and 4OHT were added to cells (Fig. 1c). We note that the ER50 DD can also be deployed to regulate the activity of catalytically inactive *Staphylococcus aureus* Cas9 (ref. 20), a Cas9 variant with distinct sgRNAs (Supplementary Fig. 5), highlighting the ready adaptability of our approach to next-generation RNA-guided, dCas9-based transcriptional activators.

Meaningful interrogation of gene function frequently requires the ability to dose-control transcript levels across a wide dynamic range. The pharmacologic chaperoning-based mechanism of DD stabilization can engender a broad range of dose control<sup>13,14</sup>. Indeed, as shown in Figure 1d, we were able to control the levels of TMP-mediated *ILIRN* mRNA induction in the DHFR-regulated PP7.VP64 transcription activation domain across orders of magnitude simply by modulating the dose of TMP. *ASCL1* mRNA upregulation was controlled across a similar range by modulation of the 4OHT dose in cells expressing the ER50.MS2.p65.HSF1 transcription activation domain (Fig. 1d). This precise tuning of transcriptional activity demanded little optimization of expression levels of dCas9, sgRNA, or transcription activation domains.

These data demonstrated ‘chemical’ control of endogenous gene transcription across several dimensions, including dose, time, and orthogonal modulation of multiple genes. Next, we sought to engineer catalytically active Cas9 variants displaying dose-dependent and

temporal control of nuclease activity and specificity. Such systems would enable regulated and specific genome editing. Temporal control of nuclease activity may also have uses in emerging technologies, including gene drives<sup>3,21</sup>. Consistent with our observations for dSpCas9.VP64 (Supplementary Fig. 1), we found that the fusion of a DHFR or ER50 DD to the N or C terminus of catalytically active SpCas9 resulted in limited small-molecule control (Supplementary Fig. 6). In contrast, fusing DHFR or ER50 DDs to both N and C termini of SpCas9 (e.g., DHFR.SpCas9.DHFR) was more successful (Supplementary Fig. 6), providing inducible control of nuclease activity. Immunoblotting illustrated the accompanying TMP- or 4OHT-dependent increases in amounts of DHFR.SpCas9.DHFR and ER50.SpCas9.ER50 protein (Supplementary Fig. 7). Furthermore, we observed strongly dose-dependent control of gene editing activity for both of our DD.SpCas9.DD constructs (Supplementary Fig. 8), with basal activity similar to that previously reported for SpCas9 regulated by intein self-splicing<sup>22</sup> (Supplementary Fig. 9).

Off-target activity of Cas9 nucleases can lead to catastrophic biological events, including chromosomal translocations<sup>23</sup>. Truncation of sgRNAs substantially enhances Cas9 specificity, and nickase variants, FokI-dCas9 nuclease, and high-fidelity Cas9 variants also offer improvements<sup>23</sup>. We anticipated that the precise regulation of Cas9 levels afforded by fusion to small-molecule-controlled DDs would allow us to titer in optimal Cas9 concentrations to maximize gene editing on-target while minimizing it off-target<sup>22,24</sup>. Indeed, we observed enhanced specificity for on-target versus known off-target sites of *VEGFA* and *EMX1* after administering optimized doses of TMP or 4OHT for the DHFR.SpCas9.DHFR and the ER50.SpCas9.ER50 systems, respectively (Fig. 2a–d, Supplementary Table 1, and Supplementary Figs. 10 and 11).

Limiting Cas9 activity to a short temporal window is another promising avenue for enhancing genome editing specificity and has been accomplished previously via the delivery of a ribonucleoprotein complex of Cas9 and sgRNA<sup>25</sup>. Using DD-regulated Cas9, one should be able to further control the size of the temporal window (as demonstrated in Fig. 1b). In the context of gene editing, this feature is illustrated by our observation that a short (6 h) pulse of TMP in U2OS.eGFP-PEST cells co-expressing DHFR.SpCas9.DHFR and eGFP-targeting sgRNAs resulted in considerably less eGFP knockout than a 48-h pulse over the same time course (Fig. 2e). We note that it is straightforward to extend our modular method to other next-generation RNA-guided endonucleases (demonstrated, for example, in Supplementary Fig. 12).

In summary, ‘chemical’ control of Cas9 endowed by DD fusion enables robust control of genome-interrogating activities across multiple dimensions, including dose, time, gene targets, and specificity. The small molecules used are inexpensive and nontoxic and display favorable pharmacologic properties, and TMP is able to cross the blood–brain barrier. Our methodology is easily transportable to other cells and to complex organisms<sup>6</sup>, enabling not just biomedical applications but also control of CRISPR-based gene drives. Finally, our modular approach should prove readily extensible to emerging next-generation RNA-guided endonucleases.

## ONLINE METHODS

### Reagents and plasmids

Trimethoprim was purchased from Alfa Aesar (J63053, 98% purity, validated by LC-MS and stabilization of a fluorescent positive control construct, DHFR.YFP). (*Z*)-4-hydroxytamoxifen was purchased from Sigma-Aldrich (H7904, 98% purity, validated by LC-MS and stabilization of a fluorescent positive control construct, ER50.YFP). Lipofectamine 2000 (Life Technologies) was used as a transfecting agent according to the manufacturer's protocol. Plasmid sequences for DD-fused Cas9 and transcription activation domain constructs are included in the Supplementary Note.

### Cell culture

All cells were cultured at 37 °C in a 5% CO<sub>2</sub> atmosphere. HEK293T cells (Life Technologies) used in transcriptional activation experiments were cultured in Dulbecco's modified Eagle's medium (DMEM) (CellGro) supplemented with 10% FBS (CellGro) and 1% penicillin–streptomycin–glutamine (CellGro). HEK293T cells used in surveyor assays and nuclease specificity experiments and U2OS.eGFP-PEST cells<sup>26</sup> stably integrated with an eGFP-PEST fusion gene were maintained in DMEM (Life Technologies) supplemented with 10% FBS, 1× penicillin–streptomycin–glutamax (Life Technologies) and 400 µg/mL of the selection antibiotic G418 (for the U2OS. eGFP-PEST cells). Cells were continuously maintained at <90% confluency. All cell lines were sourced commercially or were functionally validated. Cells were periodically tested for mycoplasma contamination using the MycoAlert PLUS Mycoplasma Detection Kit (Lonza).

### Transcription activation experiments and quantitative RT-PCR analyses

Transient transfections of HEK293T cells (750,000 cells per well in a six-well plate format) were carried out with an equivalent mass of each plasmid (dCas9, destabilized domain effector, and sgRNA) for a total mass of 5 µg of plasmid DNA. 24 h after transfection, cells were treated with the appropriate dose of DD-stabilizing small molecule(s), as indicated, for 18 h before harvesting and subsequent RNA extraction using the EZNA Total RNA Kit I (Omega). For reversibility experiments, cells were treated 24 h after transfection with 100 nM TMP for 18 h, at which point cells were treated with fresh media either containing 100 nM TMP or lacking TMP. After the media swap, cells were incubated in fresh media before harvesting and subsequent RNA extraction using the EZNA Total RNA Kit I (Omega). qPCR reactions were performed on cDNA prepared from 1,000 ng of total cellular RNA using the High-Capacity cDNA Reverse Transcription Kit (Applied Biosystems). TaqMan qPCR probes (Life Technologies; Supplementary Table 2) or other primers (Supplementary Table 3) and Fast Advanced Master Mix (Life Technologies) were used in 5-µl multiplexed reactions and 384-well format in a Light Cycler 480 II Real-Time PCR machine. All measurements were performed at least in triplicate. Data were analyzed using the LightCycler 480 Software, version 1.5 (Roche), by the  $C_t$  method: target gene  $C_t$  values (FAM dye) were normalized to *GAPDH*  $C_t$  values (VIC dye), and fold changes in target gene expression were normalized to RFP-transfected experimental controls. Analyzed data are reported as the mean ± s.d. for technical replicates, or mean ± s.e.m. for biological replicates.

### Next-generation sequencing of Cas9-mediated genome modifications

HEK293T cells (130,000 cells per well in a 24-well plate format) were transiently transfected with 400 ng of Cas9 plasmid and 100 ng of the *EMX1(1)* sgRNA expression plasmid in the presence or absence of TMP or 4OHT, as appropriate<sup>27</sup>. Transfection of an eGFP-encoding plasmid was used as a control. We extracted genomic DNA 72 h after transfection using the QuickExtract DNA extraction kit (Epicentre) by incubating the cell suspension at 65 °C for 15 min, 68 °C for 15 min, and 98 °C for 10 min. Next-generation sequencing samples were prepared via two-step PCR (Supplementary Table 4) according to a previously reported protocol<sup>28</sup>. In the first step, PCR was performed to amplify the target gene of interest and introduce adaptors. In the second step, PCR was used to attach Illumina P5 adaptors with barcodes, after which PCR products were isolated via gel purification. DNA concentrations were determined using the Qubit dsDNA HS Assay Kit (Life Technologies) and processed for NGS analysis using the MiSeq Reagent Kit v2 300 (Illumina) according to the manufacturer's protocol.

### Analysis of Cas9 nuclease activity via disruption of genomic eGFP-PEST

Approximately 200,000 U2OS.eGFP-PEST cells were nucleofected in duplicate with 500 ng of Cas9 and sgRNA expressing plasmids along with a Td-tomato-encoding plasmid using the SE Cell Line 4D-Nucleofector X Kit (Lonza) according to the manufacturer's protocol. Approximately 30,000 transfected cells per well in five replicates were plated in a 96-well plate (Corning 3904 clear-bottom) and incubated with the indicated quantities of TMP or 4OHT for 48 h. Cells were fixed using 4% paraformaldehyde, and HCS NuclearMask Blue Stain (Life Technologies) was used as the nuclear counterstaining agent. Imaging was performed with an IXM 137204 ImageXpress Automated High Content Microscope (Molecular Devices) at 4× magnification under three excitation channels (blue, green, and red) with nine acquisition sites per well. Images were analyzed in the MetaXpress software, and data were plotted using GraphPad Prism 6.

### Western blot analyses

Cells transiently expressing the different constructs were incubated in either the absence or the presence of stabilizing small molecules (TMP or 4OHT) for 24 h or with the proteasome inhibitor MG-132 for 12 h before harvesting. Cell suspensions were spun down at 1,000g for 5 min and processed according to one of two different protocols. In protocol 1 (total cell lysis), cells were resuspended in RIPA buffer (150 mM sodium chloride, 1.0% Triton X-100, 0.5% sodium deoxycholate, 0.1% sodium dodecyl sulfate, and 50 mM Tris, pH 7.5) and incubated at 4 °C for 10 min. The cell suspensions were then vortexed for 10 min at 4 °C and spun down at 16,000g for 15 min at 4 °C. The supernatant was transferred to a fresh tube and processed for immunoblotting. In protocol 2 (nuclear extraction, cell pellets were resuspended in buffer A (10 mM HEPES, pH 7.5, 50 mM NaCl, 0.5 M sucrose, 0.1 mM EDTA, 0.5% Triton X-100, and protease inhibitors) and incubated on ice for 10 min. Cell suspensions were centrifuged at 1,000g for 5 min at 4 °C and the post-nuclear supernatant was transferred to a separate tube. Cell pellets were washed once with buffer A followed by buffer B (10 mM HEPES, pH 7.5, 10 mM KCl, 0.1 mM EDTA, and 0.1 mM EGTA). Finally, the cell pellets were resuspended in buffer C (10 mM HEPES, pH 7.5, 500 mM

NaCl, 0.1 mM EDTA, 0.1 mM EGTA, 0.1% IGEPAL (NP40), and protease inhibitors) and vortexed for 15 min at 4 °C. The cell suspensions were centrifuged at 16,000g at 4 °C. The resulting nuclear extract in the supernatant was transferred to a fresh tube and processed for immunoblotting. In a typical immunoblotting protocol, 40 µg of normalized proteins were resuspended in the appropriate lysis buffer and electrophoresed on an 8% Bis-Tris gel with SDS-Tris running buffer. The protein bands were transferred to a nitrocellulose membrane and probed with anti-HSF1(c) (Abcam, ab52757; 1:100,000), anti-Cas9 (Abcam, ab191468; 1:1,000), anti-actin as a loading control for total cell lysates (Sigma, a1978; 1:10,000), and/or anti-H3K27me2 as a loading control for nuclear extracts (Cell Signaling Technologies, 9728; 1:1,000). After blocking and incubation with primary antibodies, membranes were incubated with 680-nm or 800-nm fluorophore-labeled secondary antibodies (LI-COR Biosciences; 1:10,000) before detection using a LI-COR Biosciences Odyssey Imager. Images were processed in Image Studio Lite, version 3.1.4 (LI-COR Biosciences).

### Surveyor nuclease assay

The small-molecule-mediated control of the DHFR. SaCas9.DHFR and ER50.SaCas9.ER50 gene editing systems was investigated by SURVEYOR nuclease assay<sup>29</sup>. Briefly, HEK293T cells (130,000 cells per well in a 24-well plate) were transiently transfected with 150 ng of either SaCas9 or DD.SaCas9.DD constructs (DHFR.SaCas9.DHFR or ER50.SaCas9.ER50) along with an *EXMI(7)*-targeting sgRNA-expressing plasmid. The cells were incubated with or without appropriate DD-stabilizing small molecules (TMP: 0, 50, 500, or 5,000 nM; 4OHT: 0, 10, 100, or 1,000 nM) for 72 h post-transfection at 37 °C. After cell harvesting, the genomic DNA was isolated using the QuickExtract DNA extraction kit (Epicentre). Genomic DNA was then subjected to PCR using primers corresponding to 157 bp in the *EMXI(7)* gene segment (Supplementary Table 5) and the amplicons were purified with the QIAQuick PCR purification kit. The isolated amplicons were normalized and subjected to a quick-annealing protocol (ramp 0.03 °C/s), after which they were incubated with Surveyor nuclease S (Surveyor Mutation Detection Kits, IDT) at 42 °C for 1 h. For analysis, the samples were run on a TBE gel and the cleavage bands were visualized by staining with SYBR Gold (Supplementary Fig. 12). Indel frequencies were calculated using the equation  $\text{Indel frequency} = 100(1 - (1 - ((b + c)/(a + b + c))))$ , where *a* is the intensity of the undigested PCR band and *b* and *c* are the intensities of the cleaved bands.

### Supplementary Material

Refer to Web version on PubMed Central for supplementary material.

### Acknowledgments

This work was supported by the NIH (Director's New Innovator Award 1DP2GM119162 to M.D.S.; grant 1R21AI126239-01 to A.C.), the Edward Mallinckrodt, Jr. Foundation (Faculty Scholar Award to M.D.S.), and the Burroughs Wellcome Fund (Career Award at the Scientific Interface to A.C.). C.L.M. acknowledges the National Science Foundation for a Graduate Research Fellowship. We are grateful to B. Harvey (NIDA) and to I. Slaymaker, F.A. Ran, and B. Wagner (Broad Institute) for helpful discussions. J.K. Joung (Harvard Medical School, Boston, Massachusetts, USA) provided U2OS. eGFP-PEST cells. This work is dedicated to Professor Stuart L. Schreiber on the occasion of his 60th birthday.

## References

1. Doudna JA, Charpentier E. *Science*. 2014; 346:1258096. [PubMed: 25430774]
2. Hsu PD, Lander ES, Zhang F. *Cell*. 2014; 157:1262–1278. [PubMed: 24906146]
3. Gantz VM, Bier E. *BioEssays*. 2016; 38:50–63. [PubMed: 26660392]
4. Chen B, et al. *Cell*. 2013; 155:1479–1491. [PubMed: 24360272]
5. Hilton IB, et al. *Nat Biotechnol*. 2015; 33:510–517. [PubMed: 25849900]
6. Dominguez AA, Lim WA, Qi LS. *Nat Rev Mol Cell Biol*. 2016; 17:5–15. [PubMed: 26670017]
7. Nuñez JK, Harrington LB, Doudna JA. *ACS Chem Biol*. 2016; 11:681–688. [PubMed: 26857072]
8. Nguyen DP, et al. *Nat Commun*. 2016; 7:12009. [PubMed: 27363581]
9. Oakes BL, et al. *Nat Biotechnol*. 2016; 34:646–651. [PubMed: 27136077]
10. Iwamoto M, Björklund T, Lundberg C, Kirik D, Wandless TJ. *Chem Biol*. 2010; 17:981–988. [PubMed: 20851347]
11. Miyazaki Y, Imoto H, Chen LC, Wandless TJ. *J Am Chem Soc*. 2012; 134:3942–3945. [PubMed: 22332638]
12. Banaszynski LA, Chen LC, Maynard-Smith LA, Ooi AG, Wandless TJ. *Cell*. 2006; 126:995–1004. [PubMed: 16959577]
13. Moore CL, et al. *ACS Chem Biol*. 2016; 11:200–210. [PubMed: 26502114]
14. Shoulders MD, Ryno LM, Cooley CB, Kelly JW, Wiseman RL. *J Am Chem Soc*. 2013; 135:8129–8132. [PubMed: 23682758]
15. Perez-Pinera P, et al. *Nat Methods*. 2013; 10:973–976. [PubMed: 23892895]
16. Balboa D, et al. *Stem Cell Rep*. 2015; 5:448–459.
17. Konermann S, et al. *Nature*. 2015; 517:583–588. [PubMed: 25494202]
18. Zalatan JG, et al. *Cell*. 2015; 160:339–350. [PubMed: 25533786]
19. Zetsche B, Volz SE, Zhang F. *Nat Biotechnol*. 2015; 33:139–142. [PubMed: 25643054]
20. Nishimasu H, et al. *Cell*. 2015; 162:1113–1126. [PubMed: 26317473]
21. Esvelt KM, Smidler AL, Catteruccia F, Church GM. *eLife*. 2014; 3:e03401. [PubMed: 25035423]
22. Davis KM, Pattanayak V, Thompson DB, Zuris JA, Liu DR. *Nat Chem Biol*. 2015; 11:316–318. [PubMed: 25848930]
23. Tsai SQ, Joung JK. *Nat Rev Genet*. 2016; 17:300–312. [PubMed: 27087594]
24. Zuris JA, et al. *Nat Biotechnol*. 2015; 33:73–80. [PubMed: 25357182]
25. Kim S, Kim D, Cho SW, Kim J, Kim JS. *Genome Res*. 2014; 24:1012–1019. [PubMed: 24696461]
26. Fu Y, et al. *Nat Biotechnol*. 2013; 31:822–826. [PubMed: 23792628]
27. Schneeberger K. *Nat Rev Genet*. 2014; 15:662–676. [PubMed: 25139187]
28. Hsu PD, et al. *Nat Biotechnol*. 2013; 31:827–832. [PubMed: 23873081]
29. Ran FA, et al. *Nat Protoc*. 2013; 8:2281–2308. [PubMed: 24157548]

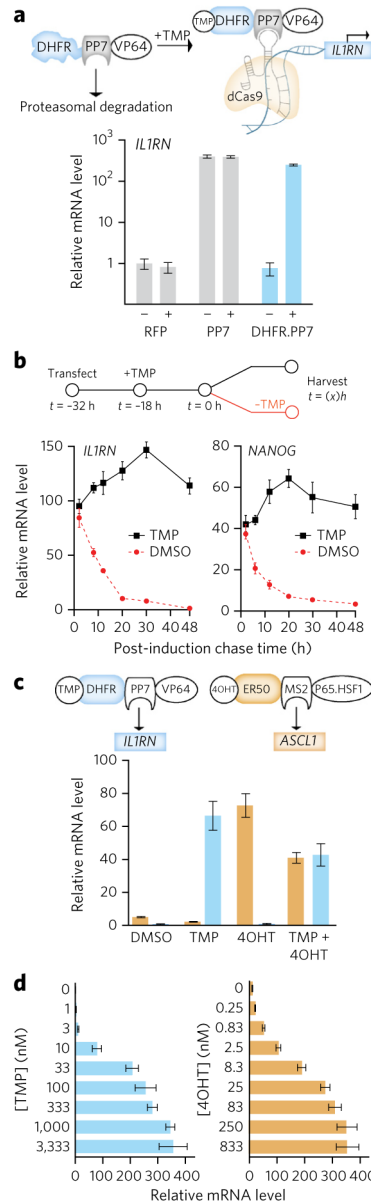


### Figure 1. Multidimensional ‘chemical’ control of endogenous transcript levels

(a) Top, small-molecule-mediated transcription induction via a destabilized domain-fused transcription activation domain (DHFR.PP7.VP64), dSpCas9, and an sgRNA. Bottom, HEK293T cells transfected with dSpCas9 and an RFP control, PP7.VP64, or TMP-regulated DHFR.PP7.VP64 targeted to *IL1RN* were treated with 10  $\mu$ M TMP for 18 h before qPCR analysis. (b) Rapid turn-off of transcription. Cells were transfected and treated with 100 nM TMP to upregulate endogenous *IL1RN* (additional biological replicates are shown in Supplementary Fig. 3) or *NANOG*. After 18 h of TMP treatment, cells were provided with fresh media containing or lacking TMP before harvesting and analysis by qPCR. (c) Independent, small-molecule-mediated control of transcript expression for two genes in cells expressing dSpCas9 and two orthogonal destabilized domain-regulated transcription activation domains. DHFR.PP7.VP64 was targeted to *IL1RN*, and ER50.MS2.p65.HSF1

was targeted to *ASCL1*. Transfected cells were treated as indicated (TMP, 100 nM; 4OHT, 10 nM) for 18 h before qPCR analysis. **(d)** Highly dose-responsive endogenous gene upregulation in cells transfected with dSpCas9, appropriate sgRNAs, and either DHFR.PP7.VP64 (left) or ER50. MS2.p65.HSF1 (right) targeted to *IL1RN* or *ASCL1*, respectively. Transfected cells were treated with increasing concentrations of TMP or 4OHT for 18 h before qPCR analysis. Error bars represent  $\pm$ s.e.m. from biological replicates ( $n = 3$ ; **a,c**) or  $\pm$ s.d. across technical replicates ( $n = 4$ ; **b,d**).

Author Manuscript

Author Manuscript

Author Manuscript

Author Manuscript

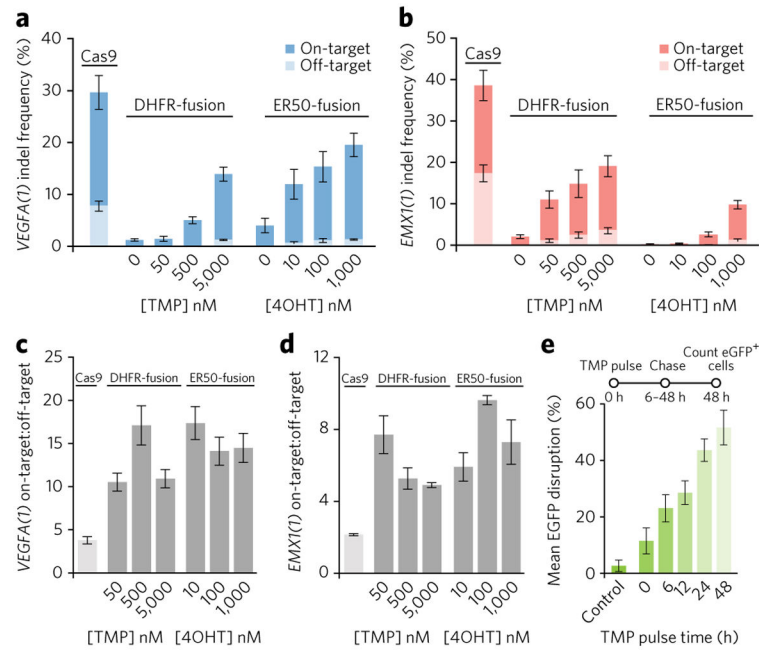


**Figure 2. Dose and temporal regulation of DD.SpCas9.DD-mediated insertion/deletion (indel) formation**

(a,b) TMP- and 4OHT-dose-dependent control of on- and off-target activity of DD.SpCas9.DD targeting *VEGFA* (a) or *EMX1* (b). HEK293T cells were transfected with SpCas9, DHFR.SpCas9.DHFR, or ER50.SpCas9.ER50 and treated as indicated with vehicle, TMP, or 4OHT for 48 h before genomic DNA extraction and analysis of on-target and off-target indel frequencies by next-generation sequencing. (c,d) Ratiometric representation of on-target:off-target indel frequencies of DD.SpCas9.DD for *VEGFA* (c) and *EMX1* (d). (e) Temporal control of DHFR.SpCas9.DHFR-mediated genome editing analyzed by an eGFP disruption assay. U2OS.eGFP-PEST cells nucleofected with a plasmid expressing DHFR.SpCas9.DHFR and an sgRNA targeting eGFP were incubated with TMP for increasing periods of time (6–48 h) before media swap to remove TMP. eGFP<sup>+</sup> cells were counted using automated, high-content imaging microscopy. Error bars represent  $\pm$ s.e.m. from biological replicates ( $n = 4$  (a–d) or 5 (e)).